

Cascades of transcriptional induction during dendritic cell maturation revealed by genome-wide expression analysis

ÖZLEM TÜRECI,¹ HONGJIN BIAN,* FRANK OLIVER NESTLE,[†] LAURA RADDRIZZANI,[‡] JAMES A. ROSINSKI,* ANATOLI TASSIS,[†] HOLLY HILTON,* MARK WALSTEAD,* UGUR SAHIN,² AND JUERGEN HAMMER*²

III. Department of Internal Medicine, University of Mainz, Germany; *Genomic and Information Sciences, Hoffmann-La Roche Inc., Nutley, New Jersey, USA; [†]Department of Dermatology, University Hospital Zürich, Switzerland; and [‡]Affymetrix, Santa Clara, California, USA

ABSTRACT Dendritic cells (DC) are central regulators of immunity. Signal-induced maturation of DCs is assumed to be the starting point for specific immune responses. To further understand this process, we analyzed the alteration of transcript profiles along the time course of CD40 ligand-induced maturation of human myeloid DCs by Affymetrix GeneChip® microarrays covering >6800 genes. Besides rediscovery of genes already described as associated with DC maturation proving reliability of the methods used, we identified clusterin as novel maturation marker. Looking across the time course, we observed synchronized kinetics of distinct functional groups of molecules whose temporal coregulation underscores known cellular events during dendritic cell maturation. For example, an early-peaking wave of inflammatory chemokines was followed by a sustained increase of constitutive chemokines and accompanied by slow but continuous induction of survival proteins. After an immediate but transient induction of cytokine-responsive transcripts, there was an increased expression of a group of genes involved in not only the regulation of cytokine effects, but also of transcription in general. Our results demonstrate that microarray studies along time courses combined with real-time PCR not only discover new marker molecules with functional implications, but also dissect the molecular kinetics of biological processes identifying complex pathways of regulation.—Türeci, O., Bian, H., Nestle, F. O., Radrizzani, L., Rosinski, J. A., Tassis, A., Hilton, H., Walstead, M., Sahin, U., Hammer, J. Cascades of transcriptional induction during dendritic cell maturation revealed by genome-wide expression analysis. *FASEB J.* 17, 836–847 (2003)

Key Words: DC • B cells • apoptotic death

DENDRITIC CELLS (DC) are professional antigen-presenting cells that play a pivotal role in the control of immunity. They are regarded as choreographers of immune responses and are involved in central and peripheral tolerance, pathogen protection, as well as anti-cancer immune responses. As immature cells spe-

cialized in antigen uptake and processing, DCs are scattered throughout the body. Upon activation with signals like CD40L or by lipopolysaccharides (LPS), interleukin 1 (IL-1), and tumor necrosis factor (TNF), they enter lymphatic vessels and travel to lymph nodes. During transit, the cells undergo functional alterations, including loss of antigen uptake and processing and an increase of accessory functions. This transforms them from being poorly immunogenic to being the most potent of all antigen-presenting cells, capable of activating naive T cells, B cells, and NK cells (1, 2). This maturation is irreversible and ends with apoptotic death (3).

DCs loaded with tumor antigens have become the centerpiece of clinical trials testing active immunotherapy strategies. Promising pilot studies have induced specific anticancer responses, including some clinical responses (4, 5). Current clinical trials are still in phase I, with many differences in study design and execution. Important variables include the source of DCs, the choice of antigens, the method of antigen loading and the route and timing of administration (6). The requirement for and the method of DC maturation are receiving particular attention. This is due to observations from in vitro studies and animal models demonstrating that mature DCs induce more potent antigen-specific T cell responses than immature DCs. Furthermore, preliminary observations in human studies suggest that immature DCs might actually down-regulate antigen-specific T cell responses but mature DCs augment them (7).

There is still much debate on how to define DC maturation, how to maintain the maturational status, and how to harmonize the route of administration with the state of the DC preparation.

The prerequisite for answering such questions is the dissection of DC maturation at the molecular level. In fact, identification of DC-associated gene products and

¹ Correspondence: III. Medizinische Klinik und Poliklinik, Johannes Gutenberg Universität Mainz, Obere Zahlbacherstr. 63, 55131 Mainz, Germany, E-mail: Tureci@mail.uni-mainz.de

² Both authors contributed equally.

maturation-induced changes has paved the way toward a better molecular understanding of dendritic cell immunobiology (8). However, how DCs undergo such dramatic and well-coordinated changes in phenotype and function is still not fully understood. Traditional experimental designs have been unable to sufficiently capture the biology of DC, given the rapid morphing of this cell type and the functional switches made during DC maturation.

Oligonucleotide microarray technology is a powerful means for systematically and extensively assessing entire transcriptomes (9). The present study was designed to explore transcriptional changes accompanying maturation of dendritic cells in response to CD40L-triggering (10) using high-density oligonucleotide arrays. To capture the sequentially changing properties of DCs during the maturation process, kinetic studies by quantitative real-time PCR were performed to identify different coregulated functional classes along the time course. Our observations provide further understanding of the biological function of DCs, allow dissection of the temporo-spatial topography of immune responses, and thus teach crucial lessons concerning design of clinical studies.

MATERIALS AND METHODS

Generation of monocyte-derived dendritic cells by culture with IL-4 and GM-CSF

Monocyte-derived dendritic cells (DCs) were generated from PBMC isolated by standard Ficoll plaque method (Pharmacia, Piscataway, NJ, USA) from buffy coats of normal unrelated healthy donors. Cells were washed twice in PBS supplemented with 1% FCS and 2 mM EDTA, and resuspended in this buffer at 5×10^8 cells/mL. PBMCs were incubated with anti-CD14 monoclonal antibody-coated microbeads (Milteny, Auburn, CA, USA) at 4°C for 15 min. Subsequently, CD14⁺ monocytes were isolated by passing the PBMCs through a magnetic cell separation either manually or with Automacs (Miltenyi). CD14⁺ monocytes were counted and assayed for viability by Trypan blue exclusion. CD14⁺ cells at 95–99% purity, as assessed by flow cytometry, were cultured for 7 days in RPMI 1640, 2 mM L-glutamine, streptomycin/penicillin, and 10% FCS supplemented with 1000 U/mL IL-4 and 1000 U/mL GM-CSF (Genzyme, Boston, MA, USA) to obtain immature dendritic cells (iDC). Every other day, 50% of the medium was removed and the same amount of fresh medium containing twice the amount of cytokines was added. To obtain mature dendritic cells (mDC), iDC (2×10^6 cells/mL) were cocultured after 5 days of differentiation in cytokine-supplemented medium with CD40L-transfected NIH3T3 cells. Cells were harvested either at day 5 before starting maturation or 2 and 40 h after the initiation of maturation for hybridization to microarrays and at time points 0 h, 3 h, and 30 h for confirmational quantitative RT-PCR. Alternatively, maturation was induced by adding soluble recombinant human CD40L (Alexis, Gruenberg, Germany) to the culture. Whereas CD40L-transfected NIH3T3 matured samples were used for studies with microarrays and quantitative real-time PCR, samples matured by recombinant sCD40L were preferred for the preparation of detailed time courses to obtain a synchronized and clear-cut induction independent from stochastic cell–cell interactions.

Flow cytometry

Analysis of cell surface antigens was performed by flow cytometry (FACScan, Becton Dickinson). Cells were washed, resuspended in PBS, added to each fluorescently labeled antibody diluted to the optimal concentration, mixed, and incubated for 20 min on ice in the dark. Labeled cells were then washed, fixed in 1% paraformaldehyde, and analyzed for fluorescence. Data analysis was based on examination of 10,000 cells/sample. Staining was performed with the following fluorescein isothiocyanate- (FITC) or phycoerythrin- (PtdEtn) labeled monoclonal antibodies: anti-CD83, anti-CD86, anti-CD14, and anti-HLA-DR (all from Becton Dickinson, Rutherford, NJ, USA). For intracellular staining with polyclonal affinity-purified rabbit-antibody against IAP-B and IAP-C (R&D Systems, Abingdon, U K), fixation was performed under permeabilizing conditions with 2% paraformaldehyde/0.1% saponin; 0.1% saponin was included in all buffers.

Immunofluorescence

Immature and mature DCs were generated as described but in chamber slides (Sigma, Munich, Germany). Before staining, cells were fixed with PBS/1% paraformaldehyde and permeabilized in 0.1% saponin/PBS. Staining of fixed cells was performed with monoclonal mouse anti-human clusterin antibody (Alexis) diluted 1:100 in PBS/2%FCS and subsequently with Cy3-conjugated anti-mouse IgG Fab fragment. For immunofluorescence analysis, cells were counterstained with Hoechst stain. Coverslips were mounted on slides in Slow-Fade (Molecular Probes, Eugene, OR, USA).

RNA extraction and labeling

Total RNA was extracted from snap-frozen human cells using “Ultraspec RNA isolation kits” (Biotecx, Houston, TX, USA) and purified using “RNeasy mini kits” (Qiagen, Valencia, CA). Five to 20 µg of total RNA was converted into double-stranded cDNA by reverse transcription (GIBCO BRL Life Technologies, Grand Island, NY, USA) using T7-T24 primer (5'-GGC CAG TGA ATT GTA ATA CGA CTC ACT ATA GGG AGG CGG (dT₂₄)). The double-strand cDNA product was cleaned up by phenol/chloroform/isoamyl extraction using phase lock gel (5 Prime-3 Prime, Inc., Boulder, CO, USA). Double-stranded cDNA was then converted into cRNA using an in vitro transcription (IVT) MEGAscript™ T7 kit (Ambion, Austin, TX, USA) and biotinylated nucleotides, as described. The IVT product was purified using RNeasy mini kits and fragmented.

Hybridization, washing and staining

Hybridization of fragmented IVT product to Affymetrix GeneChip® arrays was performed as suggested by the manufacturer (Affymetrix, Santa Clara, CA, USA). Hybridized arrays were washed with nonstringent buffer (6×SSPE, 0.01% Tween 20, 0.005% antifoam), then Stringent buffer (100 mM MES, 0.1 M Na⁺, 0.01% Tween 20). The arrays were stained with R-phycoerythrin streptavidin (SAPE, Molecular Probes, P/N S-866), the signals were amplified with goat biotinylated anti-streptavidin antibody (Vector, P/N BA-0500), and the arrays were further stained with SAPE. The commercially available Affymetrix HuGeneFL (6800 human full-length genes) array was used.

Image analysis

Each hybridized Affymetrix GeneChip® array was scanned with an argon-ion laser scanner at 570 nm (Agilent/ Af-

fymetrix, (GeneChip® version 3.1.) The initial absolute and comparison analysis were performed from images obtained from the scanned array using Affymetrix custom image analysis software.

Real-time quantitative PCR

Master 96-well plates were generated containing 5 ng/μL double-strand cDNA derived from total RNA using method described in “RNA isolation and labeling” section. Daughter plates were produced (final cDNA concentration: 40 pg/μL [200pg/well]) either manually or via robotics. Duplex real-time PCR (target gene and GAPDH as reference gene) on 96-well optical plates was performed using TaqMan® technology and analyzed on an ABI PRISM® PE7700 Sequence Detection System [Perkin-Elmer Applied Biosystems (PtdEtn), Lincoln, CA, USA], which uses the 5′ nuclease activity of Taq DNA polymerase to generate a real-time quantitative DNA analysis assay. PCR mix per well (25 μL) consisted of commercially available, premixed GAPDH TaqMan® primers/probe (PtdEtn), 900 nM each of 5′ and 3′ primers, and 200 nM TaqMan® probe from each target gene, ≈200pg cDNA and TaqMan® Universal PCR Master Mix (PtdEtn). The following PCR conditions were used: 50°C for 2 min, then 95°C for 10 min, followed by 40 cycles at 95°C/15 s and 62°C/1 min. The expression level of target gene was normalized to internal GAPDH and represented as relative Expression $E = 1/2^{-(\Delta C_t)}$, where C_t is the difference of threshold of cycle number between GAPDH and the target gene. Specific PCR primer pairs (5′, 3′) and fluorogenic probes (P) respectively were used for the following genes of interest: MIP-1a (sense GAG ACG AGC AGC CAG TGC TC, antisense GCA CAG ACC TGC CGG C, probe CCG TGT CAT CTT CCT AAC CAA GCG A), MIP-1b (sense TCT CAG CACC AAT GGG CTC, antisense GCT TCC TCG CGG TGT AAG AA, probe CCC TCC CAC CGC CTG CTG CT), MIP-2a (sense AAG GTG AAG TCC CCC GGA C, antisense GCC CATT CTT GAG TGT GGC TA, probe CCA CTG CGC CCA AAC CGA AGT C), MIP-2b (sense TGA ATG TAA GGT CCC CCG G, antisense TTC CCA TTC TTG AGT GTG GCT, probe CCC ACT GCG CCC AAA CCG AAG T), IL-8 (antisense CGT GGC TCT CTT GG CAG C, antisense TTA GCA CTC CTT GGC AAA ACT G, probe TCC TGA TTT CTG CAG CTC TGT GTG AAG GT), MGSA (sense TGA GGA GCC TGC AAC ATG C, antisense TCA TTG GCC ATT TGC TTG G, probe TCC GCC AGC CTC TAT CAC AGT GGC t), MIP-1d (sense CCA CTG GGT TTG GCA CAG A, antisense GAG TGC TCC AAG CCC AGG T, probe TGC CGC CCC TTC TTG GTG AGG), TARC (sense TCT CTG CAG CAC ATC CAC G, antisense GGG AAT GGC TCC CTT GAA G, probe ATG TGG GCC GGG AGT GCT GC), RANTES (sense GAC ACC ACA CCC TGC TGC T, antisense ATA CTC CTT GAT GTG GGC ACG, probe TGC TCA CAT TGC CCG CCC ACT G), BRUNOL-2 (sense CAA ATG CTC TCA GGT ATG GCG, antisense TGG TGC CAG CCG TGC, probe TGG CGC CAC AGG CTT GAC GAA T), IAP-B (sense GGT TGC AAG AAG AAC GAA CTT GT, antisense CAG TAC CCT TGA TTA TAC CCC TGC, probe ATC TGG TAG TAT GCC AGG AAT GTG CCC CT), IAP-C (sense GGA CAG GAG TTC ATC CGT CAA, antisense TCT CCT GGG CTG TCT GAT GTG, probe AGC CAG TTA CCC TCA TCT ACT TGA ACA GCT GC), clusterin (sense ACT ATC GCG GGT CAC CAC G, antisense ACC ACC TCA GTG ACA CCG GA, probe TTC CCA CAC TTC TGA CTC GGA CGT TCC), IRF-1 (sense CAT GGC TGG GAC ATC AAC AAG, antisense GCT TTG TAT CGG CCT GTG TGA, probe ATG CCT GTT TGT TCC GGA GCT GGG), IRF-4 (sense CAA CGC CTT ACC CTT CGC T, antisense GGG ACG TAG TCC CTC CAG C, probe AGC CCA GGT TCA CAA CTA CAT GAT GCC AC), DAPP-1 (sense CTT GAA CCC GGG AGG TGG, sense TGA CTC TGT CAC CCA GGC TAG A, probe CAC CTT CTC TGG GCA CCA AAG AAG GTT AC).

Kinesin-2 (sense AAA TCC TTT GCG TGC ATG C, antisense AGGAAAAGGTGAGCACAGCTG, probe TCA GTG ATT GTA CAT ACC TTG CCC ACT CCT AGA), MT-2 (sense CGC CGC CGG TGA CTC, antisense TGC AGC CTT GGG CAC ACT, probe CTG CTG CCC TGT GGG CTG TGC).

Computational analysis of data

Primary analysis of array data was performed using the Affymetrix GeneChip® software, resulting in parameters that were fed into our expression database and used for querying (see manufacturer for a detailed description of parameters): ‘Absolute Call’ (absent, present); ‘Difference Call’ (increased, decreased); ‘Average Difference’ (intensity); ‘Fold Change’; and ‘Sort Score’.

Cells of donors were not pooled for array analysis but processed individually.

To determine gene products with a significant increase of expression, we interrogated our data sets for an increase in ‘Average Difference’ (intensity) of at least threefold in both duplicates of at least 2 donors after 2 h and 40 h of maturation, respectively.

RESULTS

Generation of dendritic cells

Dendritic cells derived from three healthy blood bank donors (two duplicates from each) were prepared. To

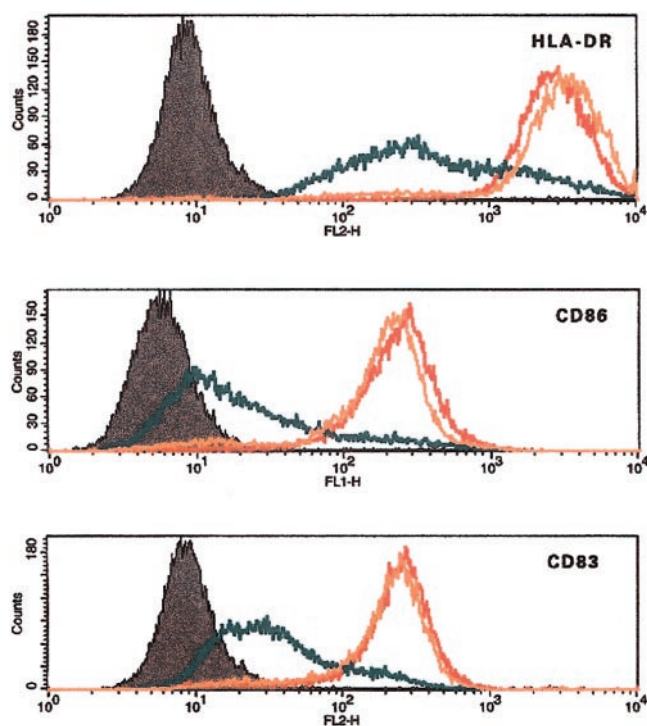


Figure 1. Flow cytometric assessment of dendritic cell (DC) maturation by staining with maturation markers CD80, CD86, and CD83. DC derived from monocytes of a healthy blood bank donor were stained after IL-4/GM-CSF supplemented culture (blue) and, after additional 30 h of cultivation with either soluble CD40L (orange) or CD40L with enhancer (red).

TABLE 1. *Transcripts increased (at least threefold) after 1 h*

Accession	Annotation	Fold of change		
		0 h/2 h	0 h/40 h	2 h/40 h
	Chemokines and receptors			
J04130	MIP1-beta	7.3	-0.3	-9.6
M69203	MCP-1	9.4	-0.6	-15.4
M23178	MIP1-alpha	5.1	-0.3	-7.1
M57731	MIP2-alpha	4.5	0.0	-4.6
X53800	MIP-2 beta	5.8	0.5	-3.6
X54489	MGSA, GRO-1	4.6	-0.2	-5.6
H54642	MIP-1 delta	46.5	65.3	0.4
AA152305	IP10	15.3	-1.2	-35.2
Y00787	IL-8	7.1	3.0	-1.0
L31584	CCR7	2.1	11.2	3.0
U64197	MIP-3a	3.8	0.2	2.9
	Cytokines, growth factors, and receptors			
X02910	TNF-alpha	22.7	0.5	-14.8
AA449789	Connective tissue growth factor	11.0	9.6	-0.1
X04602	Interleukin-6	56.9	3.2	-12.9
X04500	Prointerleukin 1 beta	183.8	32.8	-4.5
M37435	CSF-1	2.1	-0.5	-3.5
U02020	PBEF, pre-B cell colony-enhancing factor	65.0	1024.0	243.0
M29696	Interleukin-7 receptor	6.9	4.6	-0.4
T91161	Interleukin 1 receptor accessory protein, IL1RAP	13.5	5.8	-1.1
L08177	EBV induced G-protein-coupled receptor EBI2	2.5	5.0	0.7
	Cytokine response			
M92357	TNF-induced protein 2, B94	5.2	6.4	0.2
U03688	Dioxin-inducible cytochrome p450, CYP1B1	2.5	-0.1	-2.8
U52513	RIG-G, IFI 60, CiG49, IFIT4	12.8	0.0	-12.2
D28915	Hepatitis C-associated microtubular aggregate protein p44	3.1	0.0	-3.2
U50648	INF-inducible RNA-dependent protein kinase, PKR	2.1	-0.1	-2.2
M33882	IFI 78, Mx1	3.6	-1.0	-8.0
M24594	IFI 56, IFIT1	11.8	0.0	-12.3
D64110	BTG3, tob 55	2.5	1.3	-0.5
AA252606	IFI 16	6.9	-0.1	-7.3
M13755	IFI 15K	7.9	0.4	-5.3
AA143609	IFI 54, CIG42	2.4	-0.2	-2.9
W92764	TNF-inducible TSG6	89.9	55.5	-0.6
R80217	Prostaglandin-endoperoxide synthase 2, COX-2	27.8	1.1	-13.0
T92735	CIG41	24.4	-0.8	-45.3
	Survival-related proteins			
AA235874	TNF-alpha-induced protein 3, A20	96.9	126.7	0.3
U45878	MIHC, cIAP2, hIAP-1	9.3	30.4	2.1
U29680	BCL2-related protein A, BCL2A1	4.2	4.0	0.0
AF005775	FLIP, CASPER	3.3	4.1	0.2
U37547	MIHB, cIAP1, hiap-2	3.4	5.6	0.5
V00594	Metallothionein MT2A	2.2	10.5	2.7
	Processing and presentation			
AA406207	Ubiquitin hydrolyzing enzyme I, UBH1	15.6	7.7	-0.9
D86974	Beta-2 microglobulin	2.2	2.2	0.0
	Adhesion			
M24283	ICAM-1	6.0	1.9	-1.4
U72661	Ninjurin1	4.3	0.5	-2.5
HG1612-HT1612	Macmarcks, myristoylated alanine-rich C kinase substrate	2.2	17.2	4.8
	CD40 signaling			
D86968	Mitogen-activated protein kinase kinase kinase 4, MAP3K4	5.6	0.6	-3.1
M58603	NF-kappa-B	3.4	3.3	0.0
D87116	Map kinase kinase 3b	2.9	0.2	-2.3
T32837	ERK3	7.0	0.2	-5.7
M69043	I kappa B inhibitor of NF-kappa (NFKBI)	4.3	4.1	0.0
U19261	TRAF1	3.6	4.7	0.3
X75042	Rel proto-oncogene	10.2	12.1	0.2

continued on next page

TABLE 1. (continued)

Accession	Annotation	Fold of change		
		0 h/2 h	0 h/40 h	2 h/40 h
	CD			
U33017	CDw150	27.6	15.3	−0.8
M27436	CD142, tissue factor, thromboplastin	19.3	2.4	−5.1
Z11697	CD83	3.0	4.7	0.4
U30999	ALCAM, MEMD, CD166	2.1	0.3	−1.3
	Cell structure			
HG4322-HT4592	Tubulin-beta	2.5	5.5	0.9
	Phosphatases			
M93425	Protein tyrosine phosphatase, PTP-PEST	2.2	0.3	−1.4
L11329	Dual specificity phosphatase 2, DUSP2	−121.0	645.0	−22.0
AA251556	DAPP1, dual adaptor phosphotyrosine, and phosphoinositides 1	273.0	3962.0	12552.0
	Stress response			
X65965	Superoxide dismutase, SOD-2	394.0	3056.0	2513.0
J03764	Plasminogen activator inhibitor-1 gene	377.0	1630.0	922.0
U22431	Hypoxia-inducible factor 1 alpha, HIF-1alpha	149.0	552.0	524.0
AA262439	PMAIP1, phorbol-12-myristate-13-acetate-induced protein 1	229.0	3125.0	1931.0
X15183	hsp90	1445.0	5552.0	4910.0
	Miscellaneous			
L20861	wnt-5a proto-oncogene	2.7	0.8	−1.0
M16750	pim-1	4.8	5.4	0.1
HG4036-HT4306	Retinoblastoma I	150.0	520.0	345.0
D30755	Nef-associated factor 1 alpha, Naf1a	2.0	1.7	−0.1
N27159	Activin	15.4	9.0	−0.6
L78440	STAT4	5.2	1.4	−1.6
N51499	A kinase (PRKA) anchor protein 2 (AKAP2)	8.5	12.6	0.4
M72885	GOS 2	278.0	3260.0	1030.0

obtain monocytes with high purity (>95%), we preferred magnetic sorting of CD14+ cells rather than enrichment by adherence, as the latter often results in inhomogeneous cell populations. After differentiation to immature DCs and after maturation by cocultivation with NIH3T3-CD40L cells were assessed by microscopy for the typical morphological criteria. Scattergrams (side and forward scatter) were obtained by flow cytometry. These assays confirmed authenticity and purity (>95%) of the respective cell populations. Quality of maturation was assessed by surface expression of specific markers (**Fig. 1**). Immature DCs were characterized by lack of expression of CD14 and low expression of CD80, CD83, and HLA-DR. Maturation induced high levels of CD83, CD86, and HLA-DR.

Global characteristics of transcriptional alterations in dendritic cells

Choosing stringent criteria, we interrogated our microarray data sets for genes with an increase in expression level of at least threefold after 2 or 40 h of maturation.

The Change Fold was obtained by comparing the Average Differences of the group mentioned first vs. the second. Average Difference (intensity) is the GeneChip® parameter indicating the gene expression level. It represents here the average of the Average Difference values for the genes from the three donor repli-

cates for each time point. We found 175 genes increased early at 2 h and 107 genes increased after 40 h. These data were further curated and edited. First, all ESTs found to be differentially expressed were blasted against the GenBank database (<http://www.ncbi.nlm.nih.gov/Entrez>). For most of them, identity with annotated full-length sequences could be unraveled. Second, the sequence databases were accessed to evaluate all annotations for hits derived from the full-length gene as well as the EST arrays to determine redundant appearance of gene products. Eventually, 112 hits up-regulated after 2 h and 101 hits up-regulated after 40 h remained. No overlap in up-regulated genes in either time point was observed (for complete data, see supplementary **Tables 1** and **2**).

Categorization of transcripts induced significantly upon DC maturation

The majority of genes were tentatively grouped into classes based on either pathways or functional groups (see a categorized selection in Table 1, Table 2).

The most prominent increases in transcript levels were observed in the first 2 h of maturation—for example, for IL1- β (183 \times), A20 protein (97 \times), TNF-inducible factor TSG-6 (89 \times), IL-6 (56 \times), IL-1 β (56 \times), MIP1-delta (46 \times). After the first 2 h the average fold change in transcript abundance was not as high, with diubiquitin (61 \times), cIAP2 (30 \times), clusterin

TABLE 2. *Transcripts increased at least threefold after 40 h*

Accession	Annotation	Fold of change		
		0 h/2 h	0 h/40 h	2 h/40 h
	Chemokines and receptors			
D43767	TARC	1.28	6.16	2.14
M21121	RANTES	1.5	2.7	0.5
L37036	ENA-78	-0.4	8.9	12.9
L06797	CXCR4	-0.2	3.4	4.2
	Cytokines, growth factors, and receptors			
L08187	EBV-induced G-protein-coupled receptor EBI3	0.6	6.9	4.0
X17648	GM-CSF-R	0.9	2.7	1.0
Z29064	Epidermal growth factor receptor	0.2	2.2	1.6
X63131	Retinoic acid receptor	-0.2	8.3	10.5
HG544-HT544	Endothelial cell growth factor 1	0.0	11.9	11.9
Y10659	IL-13RA	0.3	4.2	3.1
	Cytokine response			
M34455	Indoleamine-pyrrole 2,3 dioxygenase, INDO	1.6	19.2	6.9
J04164	IFITM1, IFI 17	0.0	10.7	10.7
	Survival-related proteins			
J03910	Metallothionein MT1G	-0.5	17.5	26.5
V00594	Metallothionein MT2A	1.3	3.1	0.8
M10942	Metallothionein MT1E	0.9	2.1	0.7
X64177	Metallothionein MT1H	1.1	8.7	3.7
T68873	Metallothionein MT1L	1.7	54.0	19.1
T67986	Clusterin, TRPM-2, SP40-40	0.4	23.5	17.2
U37546	MIHC, cIAP2, hIAP-1	11.4	35.0	1.9
U69546	CUGBP2, ETR-3, NAPOR-2, Brunol-3	0.4	2.4	1.4
	Processing and presentation			
X57522	TAP1, RING4	0.9	2.7	0.9
N33920	Diubiquitin, UBD	2.7	60.7	15.7
	CD40 signaling			
L41690	TRADD	0.4	2.3	1.5
U59863	I-TRAF, TANK, TRAF-2	1.5	3.8	0.9
U48807	Dual specificity phosphatase 4, MKP2	1.8	7.7	2.1
AA046246	Jun dimerization protein p21SNFT	0.3	4.0	3.0
	CD			
HG3415-HT3598	Poliovirus receptor, CD155	1.9	3.2	0.5
	Cell structure			
U03057	Fascin, SNL	1.1	3.8	1.2
X15306	Neurofilament heavy polypeptide, NFH	0.1	6.5	5.7
Y08319	Kinesin heavy chain member 2, KIF2	0.8	15.6	8.3
	G-Protein signaling			
S59049	Regulator of G-protein signaling 1, RGS1, BL34, 1R20	0.9	13.3	6.7
D79990	Ras association (RalGDS/AF-6) domain family 2, RASSF2	0.2	2.7	2.1
U44103	RAB9	0.1	2.8	2.6
L13391	Regulator of G-protein signaling 2, RGS2, GOS 8	1.8	5.3	1.2
M23379	GTPase-activating protein ras p21	0.9	2.5	0.8
U02081	NET1A (guanine nucleotide regulatory protein)	0.5	5.7	3.6
	Phosphatases			
X68277	DUSP1 = dual specificity phosphatase 1	0.8	3.6	1.5
U15932	DUSP5, dual specificity phosphatase 5	1.9	6.3	1.5
M31724	Protein tyrosine phosphatase, PTP-1B	0.9	3.7	1.4
	Stress response			
X95325	CSDA (cold shock domain protein A)	0.3	2.0	1.3
M60974	Growth arrest and DNA damage-inducible GADD45A	1.5	7.1	2.2
X99050	UV radiation resistance-associated gene, UVRAG	0.2	2.1	1.5
D38551	RAD21	0.7	2.1	0.8
	Regulation			
L05072	Interferon regulatory factor 1, IRF1	1.7	3.7	0.7
U52682	Interferon regulatory factor 4, IRF4	1.3	4.4	1.3
X89750	TG interacting factor, TALE family homeobox	0.4	2.1	1.1
X79888	AU RNA binding protein, enoyl-coenzyme A hydratase	0.5	4.5	2.7
U07231	G-rich RNA sequence binding factor-1, GRSF-1	0.4	4.0	2.6
L19871	Activating transcription factor 3, ATF3	1.1	3.1	1.0

continued on next page

TABLE 2. (continued)

Accession	Annotation	Fold of change		
		0 h/2 h	0 h/40 h	2 h/40 h
	Miscellaneous			
L06633	Transcription factor PSCDBP	1.7	9.9	3.0
Y00097	Annexin VI, calelectrin	0.0	3.9	3.9
U43185	STAT 5a	1.1	2.7	0.8
M83652	Properdin P factor	1.3	6.9	2.5
X77794	Cyclin G1	0.5	2.1	1.1
U47414	Cyclin G2	0.3	4.1	2.9
U56816	Tyrosine- and threonine-specific cdc2- inhibitory kinase, MYT1	0.5	6.0	3.8
M97796	Inhibitor of DNA binding 2, Identify	1.4	3.5	0.9
L07548	Aminoacylase-1, ACY1	0.3	3.9	2.8
T56281	RNA helicase-related protein, RNAHP	2.4	19.5	5.1
X61123	BTG1, antiproliferative B cell translocation gene 1	1.4	5.9	1.9
HG2167-HT2237	A kinase (PRKA) anchor protein 13, AKAP13	0.8	2.5	0.9

(24×), and metallothionein MT1G (26×) being the most prominent ones at 40 h. Entire sets of chemokines and their receptors were found to be increased. Cytokines (IL-1 β , TNF- α , IL-6, etc.), growth factors (endothelial cell growth factor, etc.), and their receptors (IL-7R, IL-13R, GM-CSF-R, etc.) as well as accessory molecules involved in their regulation were induced. Genes related to survival, antigen processing/presentation (UBH1, TAP1, and β 2-microglobulin) and cell structure (actin bundling protein, kinesin-2, tubulin) displayed maturation-induced transcriptional increase. Other transcripts induced were clusters of differentiation such as CD83, CD150, and SLAM ligand CDw155. As expected, molecules involved in CD40 signaling were strongly induced (ERK3, MAP3K4, etc.). Transcripts such as GRSF-1, AUH, and ATF-3, which are involved in general transcriptional regulation/repression, increased along with transcripts participating in G-protein signaling (RGS1, RGS2, ras p21, etc.).

Regulated switches in expression levels of chemokines and their receptors

Since chemokines are well established as mediators of the different functional states of DCs, we sought a complete image of their time-ordered activities.

Receptors CCR7 and CXCR4 were barely detectable in immature dendritic cells but strongly up-regulated after 40 h stimulation with CD40L (Table 2).

Regarding chemokine ligands, two distinct classes of regulation were found. One class comprised chemokines with immediate induction, their expression peaking transiently after 2 h but returning to baseline or even lower levels after 40 h of maturation. These were MIP-1a, MIP-1b, MIP-2a, MIP-2b, IL-8, IP10, MIP-1d, and MGSA, most of which are known as proinflammatory chemokines (Table 1).

To confirm these data, quantitative real-time PCR

(qRT-PCR) was performed for most of these transcripts using GAPDH as reference (Fig. 2). In addition to the RNA samples hybridized to the Affymetrix GeneChip® arrays for generation of the original data sets, at least five healthy blood bank donors were screened with qRT-PCR (Fig. 2B). For some chemokines, inter-individual differences were observed in terms of baseline and peak expression levels (see data for TARC in Fig. 3 as an example), but kinetics were comparable between all individuals; data from one donor are shown (Fig. 2B).

To dissect the kinetics of induction more accurately, additional time points were included (Fig. 4). For generation of this series of samples, sCD40L was used. For all transcripts investigated, the induction kinetics observed by hybridization to the array could be confirmed by qRT-PCR and for additional donors. There were no major differences between induction by cell membrane-bound CD40L vs. recombinant soluble CD40L. For MIP-1a, MIP-2a, MIP-2b, and IL-8, peak transcript levels were reached in the first 45 min and for MIP-1b and MGSA after ~2 h. However, MIP-1d showed different kinetics, reaching its maximal transcript level after 16 h.

In contrast, TARC, RANTES, MDC, and ENA78 expression levels increased slowly in a sustained way (Fig. 2A). qRT-PCR studies confirmed these data, revealing that transcript levels of TARC and RANTES have their peaks 16 h after initiation of maturation.

Since chemokines were found to be most prominently regulated, we went back to the entire data set to review expression levels of all the chemokines or chemokine receptors represented on the array (Table 3). MCP-3, MCP-4, MIPF, and CCR1 were found to be expressed constitutively in DCs and were down-regulated strongly and rapidly upon maturation. MDC and ELC were induced, but because they do not reach high expression levels, they had escaped our initial search strategy.

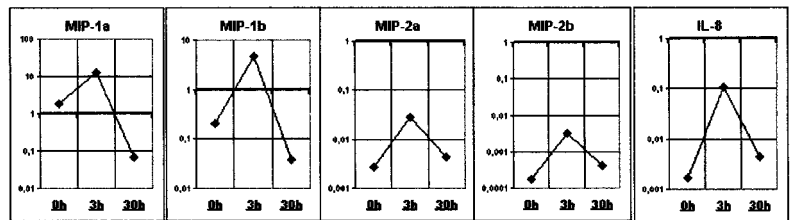
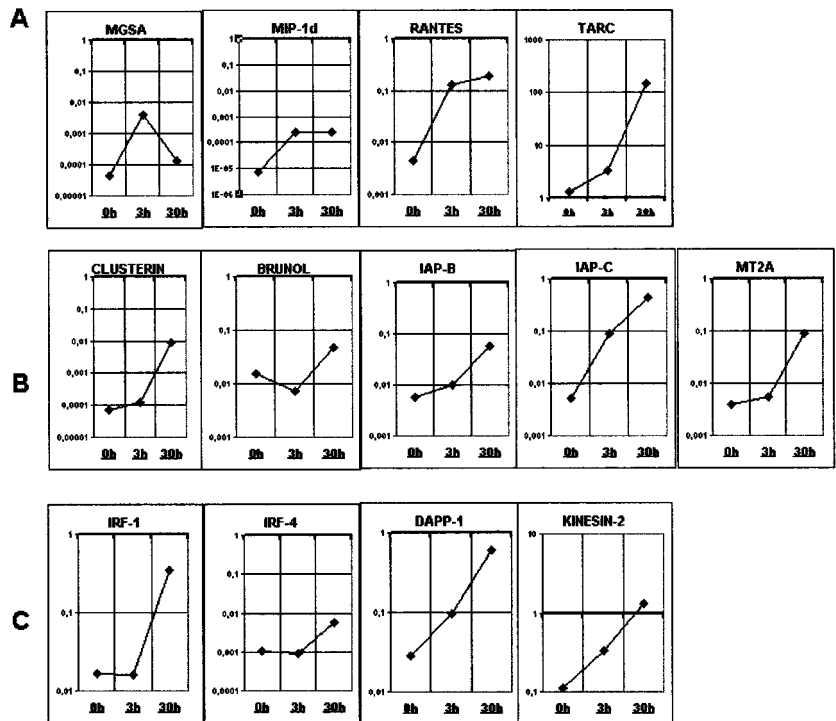


Figure 2. Transcript levels as measured by real-time PCR in dendritic cells stimulated with CD40L transfected NIH3T3 cells. Expression levels were analyzed by quantitative real-time PCR at three different time points (0, 3, 30 h) after cocubation. Data normalized for internal GAPDH expression are shown for cytokines (A), apoptosis inhibitors (B), and miscellaneous transcripts (C).



Up-regulation of a set of survival proteins in late maturation

Several molecules described as inhibiting apoptosis or protecting cells from apoptotic death were found to be induced by maturation, among them clusterin, IAP-B, IAP-B, FLIP, Brunol-3, bcl2-related protein, and several members of the metallothionein family (Tables 1, 2). For clusterin, IAPs, and Brunol-2, qRT-PCR was performed with samples from several donors, confirming the array data (Fig. 2B). Studies of kinetics by qRT-PCR revealed that the expression of these genes was induced late (Fig. 4B). In contrast to the chemokines, which had uniform kinetic patterns, different kinetics were observed for survival proteins. Brunol-2 has a steep and transient peak at 16 h whereas IAP-C is immediately but slowly increasing, reaching a plateau after 8 h. Clusterin shows a delayed induction after 4 h.

We screened the entire data set for molecules annotated as being involved in apoptosis or protection from it. We found that transcript levels of apoptosis inducing molecules such as Fas, Fas ligand, bak, bik, bax, and RAIDD were largely unaffected by maturation-induced processes (Table 3).

Though for chemokines and their receptors it is well established that regulation is centered on mRNA stability (11), this is not necessarily the case for other protein families. To confirm up-regulation of clusterin, IAP-B, and IAP-C on a protein level, we used specific antibodies. Mature dendritic cells were found to express higher amounts of both inhibitors of apoptosis compared with immature dendritic cells as revealed by flow cytometric analysis upon intracellular staining (Fig. 5). However, the extent of maturation-induced increase on the protein level was moderate compared with what was expected from RNA abundance, suggesting that protein

Figure 3. Inter-individual differences of TARC expression during maturation of dendritic cells. Analysis of DC preparations obtained from different donors demonstrated that although the baseline levels of TARC expression are different in different healthy donors, stimulation by CD40L cross-linking leads to similar relative increase of expression.

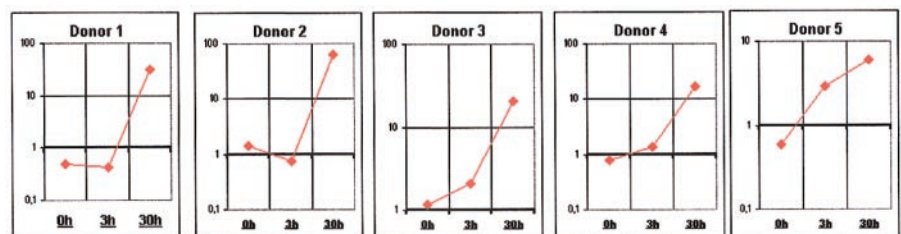
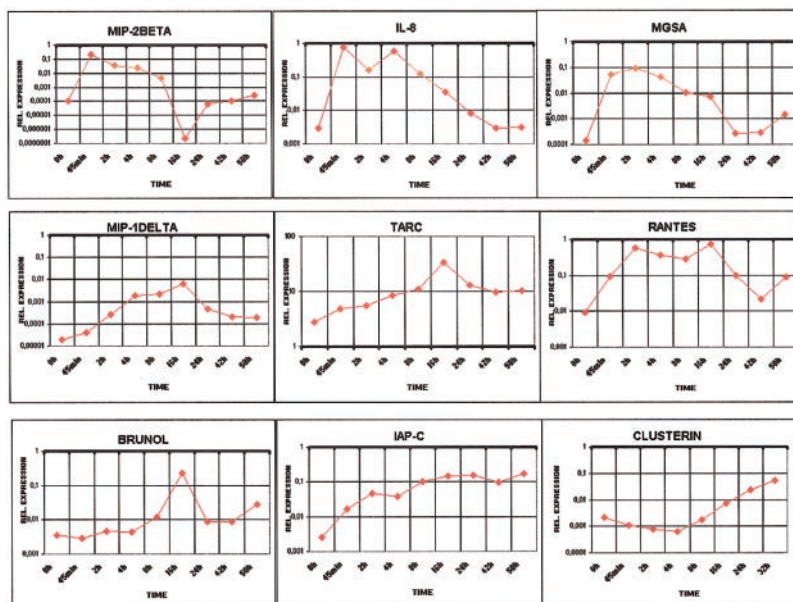


Figure 4. Transcript kinetics during dendritic cell maturation after stimulation with soluble CD40 ligand (sCD40L) by real-time PCR. The relative expression levels of chemokines MIP-1 α , MIP-1 β , MIP-2 α , MIP-2 β , MIP-1delta, IL-8, Gro- α (MGSA), RANTES, TARC, survival-related proteins clusterin, Brunol, IAP-B, IAP-C, MT2A, and regulatory factors IRF-1, IRF-4 as well as kinesin-2 and metallothionein (DAPP-1) were analyzed at 0 h, 45 min, 2 h, 4 h, 8 h, 16 h, 24 h, 42 h, 50 h after sCD40L-induced maturation of DC. Data are normalized to internal GAPDH (see Materials and Methods), whereby expression of GAPDH is 1 (boldface scale line). Samples generated from at least 5 healthy donors were analyzed. Representative examples from single individuals are shown.



turnover might be higher in mDCs. Clusterin expression as assessed by immunofluorescence microscopy was strong in a variable proportion of mDC but not detectable in iDC (**Fig. 6**). Cells show predominantly staining of the cell membrane. Occasionally, intracellular dots appeared positive.

DISCUSSION

Maturing dendritic cells were subjected to genome-wide expression profiling at three different time points to obtain “snapshots” of the course of transcriptional alterations. For 27 of 30 selected genes, array data could be confirmed by quantitative RT-PCR, suggesting that the majority of observed alterations (at least for higher fold changes) are authentic. However, qRT-PCR revealed frequently higher changes in relative expression levels than microarrays.

The exploitation of high-density oligonucleotide array technology combined with analysis of different time points opens a new dimension of understanding. Similar to viewing the entire movie in one setting instead of successively examining a few pixels at a time from each frame, this technology allows one to unravel complex inter-relationships between protagonist proteins and the theme of DC maturation (11–13). Indeed, our data reveal that entire sets of functionally related transcripts are up-regulated rather than individual transcripts only.

For example, recent studies have already implicated the involvement of chemokines and chemokine receptors in migration of DCs and their interactions with T cells (14–17). Their appearance among the significantly increased transcripts in our data not only serves as a positive control for our system, but also further refines some of the existing concepts envisioned for chemokines in the context of DC maturation.

The initial down-regulation of MCP-3, MCP-4, and

MIP-3 followed by the production of inflammatory chemokines at early time points and of constitutive chemokines later on, in concert with the respective receptors, has crucial implications for DC physiology. Inflammatory chemokines such as MIP-1 α , MIP-1 β , MIP-2 α , MIP-2 β , IL-8, MCP-1, MCP-2, MGSA, and IP-10 are expressed rapidly and at high levels (Table 1). Their expression is transient and confined to the time when DCs are supposed to still be in peripheral tissues. These inflammatory chemokines may contribute to the recruitment of immature DCs and their precursors as well as of effector cells. This is consistent with the finding that immature DCs express the inflammatory chemokine receptor CCR1 (Table 3). RANTES and MIP-1d are up-regulated with a delay and in a more sustained fashion, consistent with their role to attract T cells. Maturing DCs with up-regulated CCR7 are attracted, together with naive T and B cells, into the T cell zone by constitutively expressed chemokines such as SLC and ELC (12). Thus, rare antigen-specific T cells can be primed by Ag-loaded DCs. In a second phase, other newly arriving, Ag-bearing DCs producing chemokines such as MDC and TARC attract more efficiently activated dividing and memory T cells expressing more CCR4 than the surrounding naive T cells. Up-regulation of SDF-1 α receptor CXCR4 in maturing DC may be an additional mechanism to trap these cells in the lymph node.

Similarly, even though the role of cytokines, growth factors, and their receptors is well established in maturing DCs, our array data elucidate additional aspects by revealing sequential induction of other groups of molecules interconnected with cytokines as well as with CD40 signal transduction. A significant number of gene products increasing by at least threefold in the first 2 h are annotated as being cytokine-inducible (by either INF- γ , TNF- α , or GM-CSF), indicating immediate downstream realization of cytokine effects. It is note-

TABLE 3. Chemokines and apoptosis-related transcripts represented in the arrays

Chemokines and receptors				
Accession	Annotation	Fold of change		
		0 h/2 h	0 h/40 h	2 h/40 h
No change				
X85740	CCR-4	-0.5	-0.1	0.4
U84487	fractalkine	0.0	0.0	0.0
AB002409	SLC	0.0	0.5	0.5
U86358	TECK	0.0	0.0	0.0
Z49269	HCC-1	0.0	0.0	0.0
U03905	MCP-1	0.0	0.0	0.0
U51241	CCR-3	0.2	-0.4	-0.7
D49372	eotaxin	0.6	0.0	-0.6
Increase				
AF014958	CCRL2, CKRX	0.4	-2.9	-4.6
X99886	MCP-2	1.3	-2.6	-7.2
U83239	MDC	-0.2	1.2	1.5
U77180	ELC	0.0	2.0	2.0
Decrease				
U85767	MPIF-1	-0.1	-2.6	-2.2
L09230	CCR-1	-4.8	-4.8	0.0
U46767	MCP-4	-0.4	-3.1	-1.9
X72308	MCP-3	-3.3	-1.1	0.5

Apoptosis-related proteins				
Accession	Annotation	Fold of change		
		0 h/2 h	0 h/40 h	2 h/40 h
No change				
X89986	Bik	0.0	0.0	0.0
U66879	Bad	0.1	0.1	0.0
X84213	Bak	0.0	0.0	0.0
Z23115	Bcl-xl	0.8	0.7	0.0
U86214	caspase 10	0.0	0.0	0.0
X82279	Fas	0.0	0.0	0.0
U11821	Fas ligand	0.0	0.0	0.0
U84388	RAIDD, CRADD	-0.2	0.2	0.5
U83598	DDR3	-0.1	0.0	0.1
S78085	programmed cell death 2	0.0	0.0	0.0
U45880	XIAP	0.0	0.0	0.0
M13994	Bcl-2	-0.2	-0.2	0.0
Increase				
U37518	TRAIL	2.4	0.2	-1.8
AF006041	Daxx	0.4	1.6	0.8
U78798	TRAF6	0.6	1.0	0.3
Decrease				
U80017	SMN1, survival of motor neuron 1	-1.3	-0.1	1.1

worthy that nearly all of these follow the same pattern in which peaks are transient and transcript levels are back to baseline or below after 40 h. Despite the lack of interferon, elevation of interferon-associated genes oc-

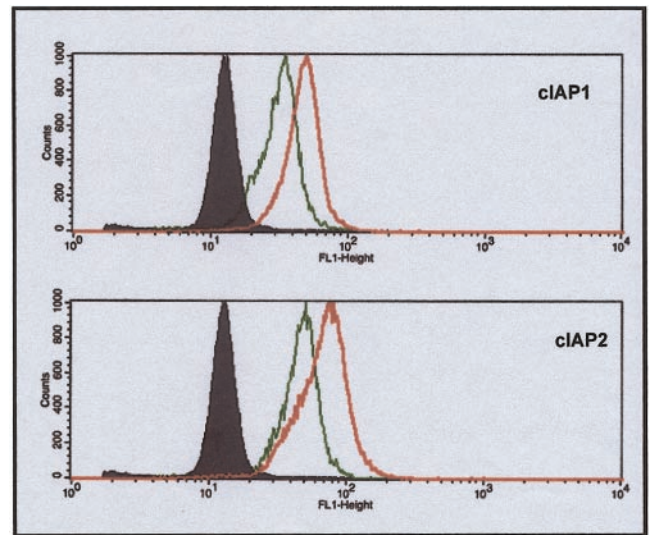


Figure 5. IAP-B and IAP-C are up-regulated in mature dendritic cells. Flow cytometric analysis of cells subsequent to intracellular staining with antibodies specific to inhibitors of apoptosis IAP-C (A) and IAP-B (B) reveals up-regulation in mature dendritic cells (red) compared with immature dendritic cells (green).

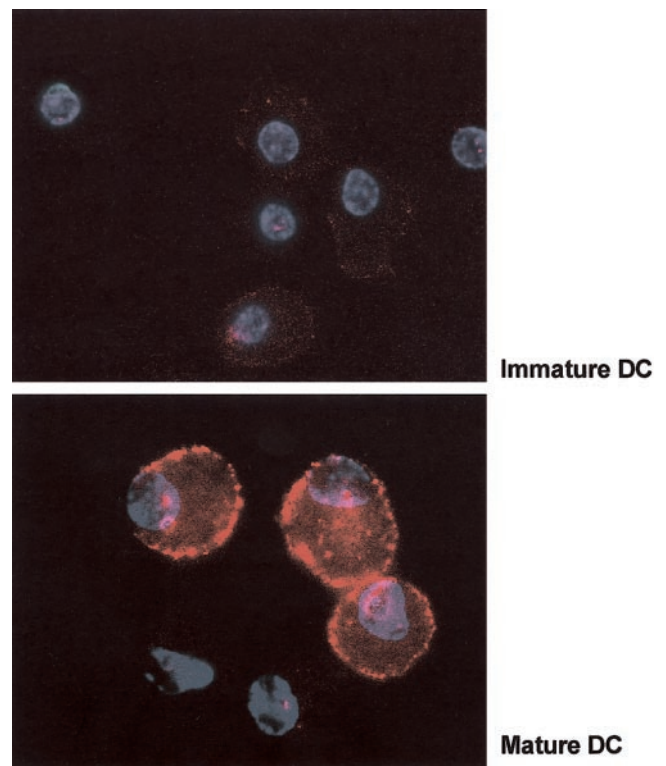


Figure 6. Clusterin is up-regulated in mature dendritic cells. Immunofluorescence microscopy using an anti-clusterin antibody visualized by a Cy3-conjugated secondary Fab fragment (red) discloses B) induction of clusterin upon maturation of dendritic cells with expression confined predominantly to the cell membrane; A) iDC do not express this gene product. Cell nuclei were counterstained with Hoechst stain.

curs since CD40 signal transduction pathway involves JAK/STAT activation. Thus, similar signaling components as with IFN- γ are recruited and similar molecular activation patterns were observed (18). After some delay, counter-regulatory events occur. IRF1 and IRF4, which are involved in regulation of JAK/STAT-mediated effects, increase (19). Also showing an increase are a TG-interacting factor that inhibits activation of the retinoic acid responsive element and AUH, which mediates fast degradation of AUUUA-rich RNAs like IL-3, granulocyte/macrophage colony-stimulating factor, c-fos, and c-myc.

DCs are thought to be short-lived (1), dying shortly after reaching the draining lymph node, thus ensuring adequate space for the constant influx of fresh DCs loaded with different antigens. However, it is also relevant that sufficient longevity and abundance of antigen-pulsed DCs are critical factors in the magnitude of a T cell response to antigen. Factors controlling DC survival are equally important for antigen-specific stimulation in the induction of immunity. It has already been reported that dendritic cells are resistant to apoptosis through Fas (20) and that CD40 ligation exerts a survival-promoting effect, presumably by up-regulation of Bcl-2 (21). Molecules such as c-FLIP (22) or T cell-produced factors like TRANCE and TNF (23–25) are reported to confer this resistance, but the molecular basis for this is not clearly understood. We report an entire set of protective molecules increasing. Among them are IAP-C (inhibitor of apoptosis C), as previously reported (26), but also IAP-B, FLIP, and clusterin.

Survival-related proteins seem to appear later in maturation, so they may not be detected in the first 6 h, as investigated by Aicher et al. (26) using Multiprobe RPA. In accord with this, several proteins inducible by different stress factors or damaging agents and with reported general protective functions are also found to be significantly increased early (SOD-2, hypoxia-inducible factor α , etc.) as well as late (RAD21, DNA damage-inducible GADD45, etc.) in maturation.

The relevance of our findings to the fate of DCs during natural immune responses in humans is so far unknown. However, monocyte-derived DCs like those in our studies are being used in clinical trials as cancer vaccines (4, 5, 27). Therefore, it is important to determine the factors promoting their survival by functional studies. There are indications that current trials operate below the adjuvant potential of DCs (28), suggesting that application of information for the elongation of DC lifespan is of high interest. Also important for immunotherapy is that treating DCs with maturation signals immediately initiates coordinated cascades of rapid molecular changes. Early on, factors contributing crucially to the successful generation of immune responses are produced. Hence, it may be an advantage to mature DCs briefly for 2 h ex vivo rather than 24–48 h and inject them at early maturation stages. The concept of dendritic cell exhaustion would also favor such a procedure (29).

A surprising observation was maturation-induced up-regulation of clusterin in dendritic cells. Clusterin has been implicated in a variety of functions such as lipid transport, reproduction, cell–cell interaction, complement regulation, tissue remodeling, and cell survival (30, 31). Initially it was believed to be proapoptotic because of its accumulation in tissues undergoing apoptosis. The observation of clusterin accumulating in the surviving cells adjacent to the apoptotic led to reassessment of its role in apoptosis (32). According to recent studies, clusterin has been implied in cytoprotection of vital cells, presumably by assisting in the clearance of apoptotic vesicles and membrane remnants. Clusterin seems to act as adaptor between apoptotic phosphatidylserine-coated vesicles and its high-affinity receptor gp330/megalin. Moreover, clusterin was assigned potent chaperone-like activities, protecting a wide range of proteins from denaturation (33). Recent data suggest that clusterin is a novel type of secreted extracellular heat shock protein (34). Recently, clusterin was suggested as a diagnostic marker for anaplastic large cell lymphomas by microarray studies (35). Performing immunohistochemistry on primary lymphoid neoplasms, Wellmann et al. (35) not only observed strong staining of ALCL cells but also of follicular dendritic cells. This confirms that not only dendritic cells generated in vitro from monocytes, but also dendritic cells in situ, express clusterin. Ongoing studies are needed to evaluate clusterin function in the context of mature dendritic cells.

Besides known genes that have not been identified as involved in DC maturation before (Tables 1 and 2), yet unclassified genes represented by ESTs and genomic clones have been observed to be differentially expressed. Determination of their identity and analysis of their function may reveal novel aspects.

In summary, we have reported that global transcript analysis by microarrays in combination with kinetics analysis of single transcripts is a powerful new tool that will aid in developing a more comprehensive understanding of dendritic cell maturation. We not only elucidated functional networks of molecules and temporal relationships between classes of transcripts; we were able to identify differentially expressed gene products including clusterin, which we suggest as a new marker for dendritic cell maturation. **FJ**

We wish to thank Dr. Christoph Huber for his continuous support and encouraging discussions. Ö.T. and U.S. were supported by the Deutsche Forschungsgemeinschaft (Tu 115/1–2 and D1/SFB 432).

REFERENCES

1. Banchereau, J., and Steinman, R. M. (1998) Dendritic cells and the control of immunity. *Nature (London)* **392**, 245–252
2. Hart, D. N. (1997) Dendritic cells: unique leucocyte populations which control the primary immune response. *Blood* **90**, 3245–3287
3. Winzler, C., Rovere, P., Rescigno, M., Granucci, F., Penna, G., Adorini, L., Zimmermann, V. S., Davoust, J., and Ricciardi-

- Castagnoli, P. (1997) Maturation stages of mouse dendritic cells in growth-factor dependent long-term cultures. *J. Exp. Med.* **185**, 317–328
4. Nestle, F. O., Aljagac, S., Gilliet, M., Sun, Y., Grabbe, S., Dummer, R., Burg, G., and Schadendorf, D. (1998) Vaccination of melanoma patients with peptide- or tumor lysate-pulsed dendritic cells. *Nat. Med.* **4**, 328–332
5. Thurner, B., Haendle, I., Roder, C., Dieckmann, D., Keikavoussi, P., Jonuleit, H., Bender, A., Maczek, C., Schreiner, D., von den Driesch, P., et al. (1999) Vaccination with mage-3A1 peptide-pulsed mature, monocyte-derived dendritic cells expands specific cytotoxic T cells and induces regression of some metastases in advanced stage IV melanoma. *J. Exp. Med.* **190**, 1669–1678
6. Nestle, F. O., Banchereau, J., and Hart, D. (2001) Dendritic cells: On the move from bench to bedside. *Nat. Med.* **7**, 761–765
7. Dhodapkar, M. V., and Steinman, R. M. (2002) Antigen-bearing immature dendritic cells induce peptide-specific CD8(+) regulatory T cells in vivo in humans. *Blood* **100**, 174–177
8. Hartgers, F. C., Figdor, C. G., and Adema, G. J. (2000) Towards a molecular understanding of dendritic cells immunobiology. *Immunol. Today* **21**, 542–545
9. Lockhart, D. J., Dong, H., Byrne, M. C., Follettie, M. T., Gallo, M. V., Chee, M. S., Mittmann, M., Wang, C., Kobayashi, M., Horton, H., et al. (1996) Expression monitoring by hybridization to high-density oligonucleotide arrays. *Nat. Biotechnol.* **14**, 1675–1680
10. van Kooten, C., and Banchereau, J. (1997) Functions of CD40 on B cells, dendritic cells and other cells. *Curr. Opin. Immunol.* **9**, 330–337
11. Granucci, F., Vizzardelli, C., Virzi, E., Rescigno, M., and Ricciardi-Castagnoli, P. (2001) Transcriptional reprogramming of dendritic cells by differential stimuli. *Nat. Immunol.* **2**, 882–888
12. Granucci, F., Vizzardelli, C., Pavelka, N., Feau, S., Persico, M., Virzi, E., Rescigno, M., Moro, G., and Ricciardi-Castagnoli, P. (2001) Inducible IL-2 production by dendritic cells revealed by global gene expression analysis. *Nat. Immunol.* **2**, 882–888
13. Huang, Q., Liu, D., Majewski, P., Schulte, L. C., Korn, J. M., Young, R. A., Lander, E. S., and Hachohen, N. (2001) The plasticity of dendritic cell responses to pathogens and their components. *Science* **294**, 870–875
14. Dieu, M. C., Vanbervliet, B., Vicari, A., Bridon, J. M., Oldham, E., Ait-Yahia, S., Briere, F., Zlotnik, A., Lebecque, S., and Caux, C. (1998) Selective recruitment of immature and mature dendritic cells by distinct chemokines expressed in different anatomic sites. *J. Exp. Med.* **188**, 373–386
15. Sallusto, F., Schaerli, P., Loetscher, P., Schaniel, C., Lenig, D., Mackay, C. R., Qin, S., and Lanzavecchia, A. (1998) Rapid and coordinated switch in chemokine receptor expression during dendritic cell maturation. *Eur. J. Immunol.* **28**, 2760–2769
16. Sozzani, S., Allavena, P., D'Amico, G., Luini, W., Bianchi, G., Kataura, M., Imai, T., Yoshie, O., Bonecchi, R., and Mantovani, A. (1998) Differential regulation of chemokine receptors during dendritic cell maturation: a model for their trafficking properties. *J. Immunol.* **161**, 1083–1086
17. Cyster, J. G. (1999) Chemokines and the homing of dendritic cells to the T cell areas of lymphoid organs. *J. Exp. Med.* **189**, 447–450
18. Gupta, S., Xia, D., Jiang, M., Lee, S., and Pernis, A. B. (1998) Signaling pathways mediated by the TNF- and cytokine-receptor families target a common cis-element of the IFN regulatory factor 1 promoter. *J. Immunol.* **161**, 5997–6004
19. Yamagata, T., Nishida, J., Tanaka, S., Sakai, R., Mitani, K., Yoshida, M., Taniguchi, T., Yazaki, Y., and Hirai, H. (1996) A novel interferon regulatory factor family transcription factor ICSAT/Pip/LSIRF, that negatively regulates the activity of interferon-regulated genes. *Mol. Cell. Biol.* **16**, 1283–1294
20. Ashanasy, D., Savir, A., Bhardway, N., and Elkon, K. B. (1999) Dendritic cells are resistant to apoptosis through the FAS (CD95/APO-1) pathway. *J. Immunol.* **163**, 5303–5311
21. Björck, P., Banchereau, J., and Flores-Romo, L. (1997) CD40 ligation counteracts Fas-induced apoptosis of human dendritic cells. *Int. Immunol.* **9**, 365–372
22. Perlman, H., Pagliari, L. J., Geoorganas, C., Mano, T., Walsh, K., and Pope, R. M. (1999) FLICE-inhibitory protein expression during macrophage differentiation confers resistance to FAS-mediated apoptosis. *J. Exp. Med.* **190**, 1679–1688
23. Josien, R., Hong-Li, L., Inguli, E., Sarma, S., Wong, B. R., Vologodskaya, M., Steinman, R. M., and Choi, Y. (2000) TRANCE, a tumor Necrosis factor family member, enhances the Longevity and adjuvant properties of dendritic cells in vivo. *J. Exp. Med.* **191**, 495–501
24. Wong, B. R., Joisien, R., Lee, S. Y., Sauter, B., Li, H. L., Steinman, R. M., and Choi, Y. (1997) TRANCE (tumor necrosis factor (TNF) related activation induced cytokine), a new TNF family member predominantly expressed in T cells, is a dendritic cell-specific survival factor. *J. Exp. Med.* **286**, 2075–2080
25. Anderson, D. M., Maraskovsky, E., Billingsley, W. L., Dougall, W. C., Tometsko, M. E., Roux, E. R., Teepe, M. C., DuBose, R. F., Cosman, D., and Galibert, L. (1997) A homologue of the TNF receptor and its ligand enhance T-cell growth and dendritic cell function. *Nature (London)* **390**, 175–179
26. Aicher, A., Shu, G. L., Magaletti, D., Mulvaney, T., Pezzutto, A., Craxton, A., and Clark, E. A. (1999) Differential role for p38 mitogen-activated protein kinase in regulating CD40-induced gene expression in dendritic and B cells. *J. Immunol.* **163**, 5786–5795
27. Steinman, R. M., and Dhodapkar, M. (2001) Active immunization against cancer with dendritic cells: the near future. *Int. J. Cancer* **94**, 459–473
28. Morse, M. A., Coleman, R. E., Akabani, G., Niehaus, N., Coleman, D., and Lyster, H. K. (1999) Migration of human dendritic cells after injection in patients with metastatic malignancies. *Cancer Res.* **59**, 56–58
29. Langenkamp, A., Messi, M., Lanzavecchia, A., and Sallusto, F. (2000) Kinetics of dendritic cell activation: impact on priming of TH1, TH2 and nonpolarized T cells. *Nat. Immunol.* **1**, 311–316
30. Rosenberg, M. E., and Silksens, J. (1995) Clusterin: Physiologic and pathophysiologic considerations. *Int. J. Biochem. Cell Biol.* **27**, 633–645
31. Koch-Brandt, C., and Morgan, C. (1996) Clusterin: a role in cell survival in the face of apoptosis? *Prog. Mol. Subcell. Biol.* **16**, 130–149
32. French, L. R., Wohlwend, A., Sappino, A. P., Tschopp, J., and Schifferli, J. A. (1994) Human clusterin gene expression is confined to surviving cells during in vitro programmed cell death. *J. Clin. Invest.* **93**, 877–881
33. Viard, I., Wehrli, P., Jornot, L., Bullani, R., Vechietti, J. L., Schifferli, J. A., Tschopp, J., and French, L. E. (1999) Clusterin gene expression mediates resistance to apoptotic cell death induced by heat shock and oxidative stress. *J. Invest. Dermatol.* **112**, 290–296
34. Poon, S., Easterbrook-Smith, S. B., Rybchyn, M. S., Carver, J. A., and Wilson, M. R. (2000) Clusterin is an ATP-independent chaperone with very broad substrate specificity that stabilizes stressed proteins in a folding-competent state. *Biochemistry* **39**, 15953–15960
35. Wellmann, A., Thieblemont, C., Pittaluga, S., Sakai, A., Jaffe, E. S., Siebert, P., and Raffeld, M. (2000) Detection of differentially expressed genes in lymphomas using cDNA arrays: identification of clusterin as a new diagnostic marker for anaplastic large-cell lymphomas. *Blood* **96**, 398–404

Received for publication July 30, 2002.
Accepted for publication December 17, 2002.